JACS
JOURNAL OF THE AMERICAN CHEMICAL SOCIETY

Communication

pubs.acs.org/JACS

Creating Extremely Asymmetric Lamellar Structures via Fluctuation-Assisted Unbinding of Miktoarm Star Block Copolymer Alloys

Weichao Shi,[†] Andrew L. Hamilton,[†] Kris T. Delaney,[†] Glenn H. Fredrickson,*[,†,‡] Edward J. Kramer,[†,‡,§,△] Christos Ntaras,[#] Apostolos Avgeropoulos,*[,#] and Nathaniel A. Lynd[⊥,¶]

[†]Materials Research Laboratory, [‡]Department of Chemical Engineering, [§]Department of Materials, University of California at Santa Barbara, Santa Barbara, California 93106, United States

[#]Department of Materials Science and Engineering, University of Ioannina, University Campus, Ioannina, Greece 45110

[⊥]McKetta Department of Chemical Engineering, University of Texas at Austin, Austin, Texas 78712, United States

[¶]Materials Sciences Division, Lawrence Berkeley National Laboratory, Berkeley, California 94720, United States

Supporting Information

ABSTRACT: We report the creation of highly asymmetric lamellar structures with a well-designed miktoarm star block copolymer of the $S(IS')_3$ type, where S and S′ are polystyrenes of different lengths and I is poly(isoprene). The domain spacing can be tuned continuously from 37 nm to over 300 nm when the miktoarm star block copolymer is blended with suitable molecular weight polystyrene homopolymers. Beyond the unbinding transition of the lamellar phase, extremely asymmetric lamellar structures were obtained with up to 97 wt % polystyrene, remarkably leaving the poly(isoprene) layers intact at only 3 wt %!

As one of the basic segregation states in block copolymer self-assembly, lamellae with tunable domain periods have attracted considerable interest in a range of emerging applications.[1−7] For example, the optical band gap of lamellar photonic crystals can be significantly shifted by swelling/shrinking one layer,[3−6] and adaptive domain spacing has proven advantageous to transfer printing techniques for micro/nanodevice fabrication.[1,2,7] However, for traditional linear AB or symmetric ABA block copolymers, it is well-known that lamellar structures only form when the volume fractions of the A and B segments are nearly equal.[8−12] The available composition range for lamellae is usually located from 35% to 65% (by volume) in the strong segregation regime.[10,12] At higher or lower compositions, order−order transitions (OOTs) intervene, producing nonlamellar self-assembled structures such as double gyroid, hexagonal cylinders, and BCC or FCC spheres. The restricted composition range in conventional AB or ABA copolymers produces nearly symmetric A and B lamellar layers, which can be limiting in applications where highly asymmetric lamellae are desired.

A traditional method to achieve dissimilar layer thickness is by selectively swelling one domain with a compatible component, e.g. the A layers in an AB lamellar structure can be swollen with A homopolymer.[13−17] However, this strategy is essentially limited by a nearby OOT of the neat block copolymer, and only low molecular weight homopolymers can be utilized. Incorporation of long homopolymers in the block copolymer leads to macrophase separation at low content of homopolymer.[15−17] There have also been attempts at creating more asymmetric lamellae using block copolymer blends with additional tunable parameters, such as hydrogen-bonding interaction or dispersity (sometimes referring to cosurfactant effects).[18−21] For example, two block copolymers with equal length A blocks but unequal length B blocks are combined to form a common mixed lamellar phase, where the bidisperse B blocks occupy more relaxed conformations in the B nanolayers. This stabilizes the lamellar structure to significantly asymmetric compositions approaching 80 wt % of the majority (B) component. A similar approach could in principle be realized in BAB triblocks with unequal B end block lengths.[10] Even more significant asymmetric shifts in phase boundaries have been noted in recent years in the context of miktoarm star block copolymers.[22−28]

Here we exploit an unusual miktoarm architecture and extend it by blending with homopolymer to create equilibrium lamellar microphases with unprecedented compositional asymmetry. We leverage recent theoretical[27] and experimental work[28] demonstrating that radial "miktoarm" star block copolymers with the architecture $A(BA')_n$, $n > 1$, and the molecular weight of the A block being approximately 8 times larger than the otherwise identical A′ blocks, exhibit extreme deflections of phase boundaries in favor of A/A′ discrete and B continuous morphologies. In the particular polystyrene (S) and poly(isoprene) (I) miktoarm realization considered here, namely $S(IS')_n$, this implies the potential for lamellar phases at exceptionally large polystyrene weight fractions.[28] We further demonstrate that the asymmetry of the lamellae can be pushed to the extreme by blending a lamellar-forming $S(IS')_3$ miktoarm block copolymer with a suitable polystyrene homopolymer (hPS). Extremely asymmetric lamellar structures were obtained with up to 97 wt % polystyrene, remarkably leaving the I layers intact at only 3 wt % poly(isoprene)!

The $S(IS')_3$ miktoarm block copolymer studied exhibits a long S block (81.5 kg/mol) with one end grafted onto three IS′ diblock strands at the I terminus. Each IS′ strand has a 17.1 kg/mol I block and an 11.0 kg/mol short S′ block. The material

Received: March 19, 2015
Published: April 27, 2015

DOI: 10.1021/jacs.5b02881
J. Am. Chem. Soc. 2015, 137, 6160−6163

was prepared via anionic polymerization leading to a final dispersity of 1.03. The weight fraction of S determined from ^{1}H NMR is approximately 70 wt %, which corresponds to 67 vol %. The details concerning the materials and the sample preparation methods are described in the Supporting Information (Parts A and B).

The morphology of the neat miktoarm block copolymer is itself asymmetric lamellar, which was predicted and confirmed in our previous work.[28] Due to the unusual molecular architecture of $S(IS')_3$, the phase diagram is highly asymmetric since it combines SI_3 junctions and a bimodal distribution of polystyrene block lengths (S and S′). Indeed, our earlier self-consistent field theory (SCFT) simulations suggest that the lamellar morphology for such molecules can persist up to 81 vol % of PS (combined contribution of S and S′ blocks).[27]

To further extend the S layer thickness, we blended the $S(IS')_3$ copolymer with polystyrene homopolymer (hPS) having a range of molecular weights. The phase diagram is shown in Figure 1. Blending with short hPS molecules (20.8 and 44.6 kg/mol) leads to order−order transitions (OOTs) when the hPS content exceeds approximately 40 wt % (equivalent to 82 wt % S in total) (Supporting Information: Part C). We note that this boundary is actually close to the upper composition limit for the lamellar structure in a neat miktoarm star block copolymer.[26,27] At higher hPS compositions, a disordered structure with discrete micelles is observed. In the opposite limit of long hPS molecules (136 kg/mol), the lamellar structure is stable to just beyond 50 wt % hPS, after which macrophase separation is observed (Supporting Information: Part D). At intermediate hPS molecular weights, extreme deflection of the lamella/micelle boundary toward high hPS contents is observed, with the layers remaining intact even though they proliferate defects and eventually unbind at high hPS fraction, losing their quasi-long-range orientational order.[16,29] The extreme limit of unbound lamellae is found to be just beyond 90 wt % hPS, which is equivalent to 97 wt % S in total, much higher than the lamellar boundary in the neat miktoarm star block copolymer and well beyond the observation of lamellar order in any copolymer system or blend to date!

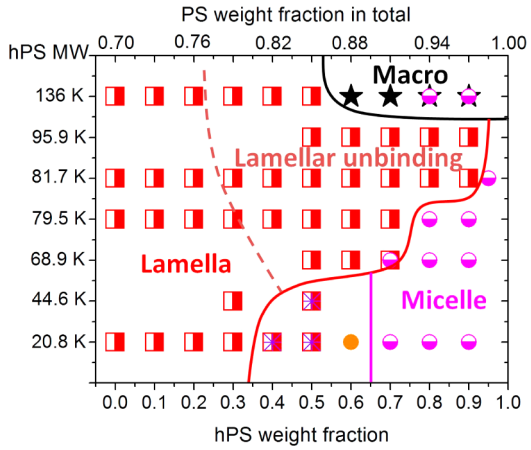

Figure 1. Phase diagram of $S(IS')_3$ blended with hPS. The half-filled squares indicate a lamellar structure; the half-filled purple circles denote a micellar structure, where I resides in the cores of micelles in a polystyrene matrix without long-range order; the black asterisks correspond to macrophase separation, where an hPS-rich macrophase coexists with a swollen lamellar phase. The small region at low hPS molecular weight between the lamellar and micellar regions involves mixed structures via OOTs, which cannot be clearly identified via TEM or SAXS. The dashed line was calculated by SCFT as described in the text; to the right positional and orientational lamellar order is disrupted by defects and eventual unbinding of lamellae.

Figure 2 shows the lamellar structures obtained in the miktoarm star block copolymer and hPS (81.7 kg/mol) blends.

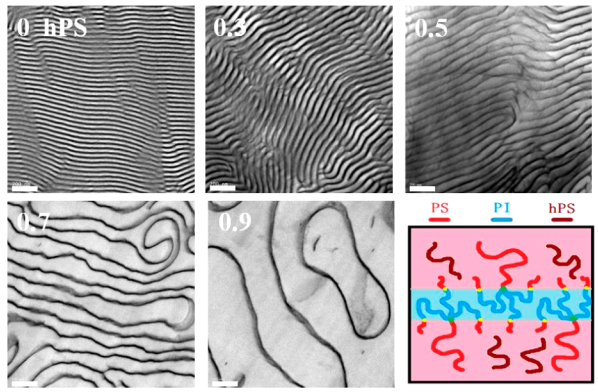

Figure 2. Morphologies observed in blends of miktoarm copolymer and hPS (81.7 kg/mol) polymer blends at different hPS weight fractions. The contrast of the TEM images is produced by staining the I domains with OsO_4 vapors resulting in those domains appearing dark. The scale bars correspond to 200 nm. The scheme shows the block arrangement near the interface.

There are two qualitative points to be gleaned from the TEM images: (1) The S domain thickness increases dramatically by the homopolymer addition. At low hPS fractions, the domain size is still on the scale of 10 nm, while at the highest S fractions, the unbinding transition gives rise to S domain thicknesses on the order of 200 nm. (2) The interfaces remain sharp across the full range of hPS contents, although more defects and layer undulation are observed at high hPS loading.

The asymmetric lamellar structures were further confirmed by small angle synchrotron X-ray scattering (Supporting Information: Part E). The unbinding of the lamellar structure can be more clearly revealed by plotting the domain period D ($D = 2\pi/q^*$, where q^* is the primary peak position) against hPS weight fraction. By assuming that the hPS is located entirely within the PS domains and does not perturb block conformations, then the thickness of the PI layers is independent of the hPS fraction used in each case. In such a case the domain period can be described by the equation (purple curve in Figure 3a):

$$D = D_0(1 - f_{0,PS})/(1 - f_{PS+hPS}) \quad (1)$$

where f_{PS+hPS} is the total volume fraction of S, D_0 is the lamellar period of the neat miktoarm star block copolymer, and $f_{0,PS}$ is the S volume fraction in the neat miktoarm, which is approximately 0.67 as stated above. Evidently this relationship holds well for the lamellar regions of the blends with the three highest molecular weight hPS. In blends with the shortest hPS (20.8 kg/mol), we observe that the OOT produces a plateau in the domain spacing, while the domain spacing increases rapidly when the hPS fraction is above 40 wt % in the high molecular weight hPS blends. The I layer thickness is constant at 13 nm for all hPS compositions while the S layers vary from 20 to 200 nm (Supporting Information: Part F), which afford a flexible domain gap variation for future applications. Notably,

DOI: 10.1021/jacs.5b02881
J. Am. Chem. Soc. 2015, 137, 6160−6163

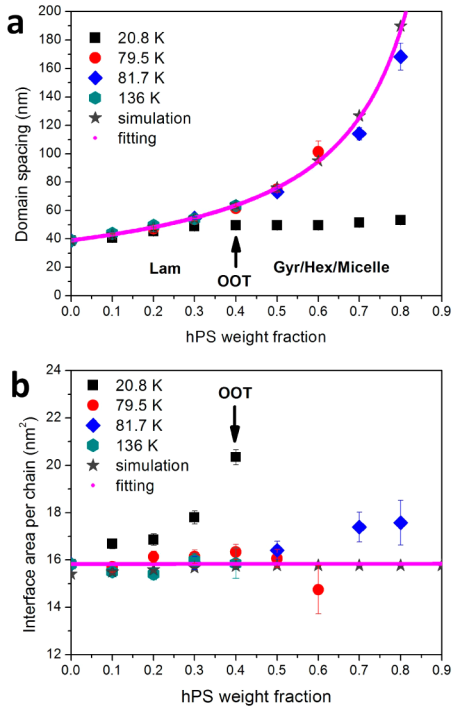

Figure 3. (a) Domain periods at different hPS weight fractions and for varying hPS molecular weights; (b) The interfacial area occupied by each miktoarm star block copolymer molecule at different hPS weight fractions. The purple curve in each figure was calculated according to eqs 1 and 2, respectively, and the stars were obtained from 1D SCFT simulations of perfect lamellar phases.

throughout the entire series, the interfacial thickness between S and I domains is nearly independent of the hPS content and was calculated to be approximately 3 nm (Supporting Information: Part G).

To supplement these experimental findings, a self-consistent field theory (SCFT) simulation study of the system was performed. Details of the implementation can be found elsewhere (Supporting Information: Part H).[30,31] Using unit cell calculations in one dimension, the free energy was minimized with respect to the domain spacing, while implicitly restricting the morphology to defect-free periodic lamellae. The lamellar domain spacings obtained from SCFT (stars in Figure 3a) confirm the trend seen from the SAXS data, lining up closely with eq 1. However, the SCFT simulations predict macroscopic instability, resulting in coexisting lamellar and disordered phases, beyond the dashed curve in Figure 1. The SCFT domain spacing data in Figure 3a at hPS fractions beyond that boundary reflect the period of a metastable mixed lamellar state. Due to its mean-field character, SCFT evidently makes an incorrect prediction of macroscopic phase separation near the dashed boundary in Figure 1, whereas thermal fluctuations cause a proliferation of defects in the swollen lamellar state of the experimental system and destroy the quasi-long-range positional order of the layers at intermediate hPS content. The remaining orientationally ordered defective layered system then unbinds its lamellae at higher hPS fractions, resulting in a loss of quasi-long-range orientational order, before any macroscopic phase separation can take place. The loss of positional order appears to coincide roughly with the dashed (SCFT macrophase separation) curve in Figure 1. Remarkably, the lamellae remain intact to very high hPS fractions after unbinding and before breaking up to micelles. This smectic-nematic–isotropic scenario has similarities to the hypothesized melting sequence of smectic-A liquid crystals[32] or unbinding phospholipid membranes,[33] but the transition here is driven not thermally, but by hPS addition, and the persistence of the layers is to our knowledge without precedent.

The equilibrium domain structure in a block copolymer melt is the result of competition between block conformational entropy and the AB interfacial tension. In traditional AB or ABA triblock copolymers, lamellae form near the symmetric composition (approximately 35 vol % to 65 vol % of either block).[9−11] Highly asymmetric lamellae are not stable due to entropy loss from the crowded long blocks. Instead, long blocks prefer to sustain a continuous matrix by confining short blocks to discrete domains. In the specific architecture of $S(IS')_3$ miktoarm star block copolymers, the crowding of the short rubbery I blocks is enhanced, which resists bending toward the I domains. Meanwhile, the S block domain behaves like a bidisperse S brush in which the crowding of the long S block is relieved by dilution of the shorter S′ blocks.[34] These dual effects make the lamellar structure stable at highly asymmetric compositions.[28] For the present miktoarm/hPS blends, the bidisperse S brush can further be characterized as either "wet" or "dry", according to its ability to be penetrated by hPS and depending on the hPS chain length relative to the S and S′ block lengths.[17]

Insight into the penetration of hPS into the S/S′ block brush presented by the miktoarm block copolymer can be obtained by computing the average area σ per block copolymer chain at the lamellar interface, which is expressed by the following equation:

$$\sigma = 2V_{PI}/(Df_{PI}) \quad (2)$$

Here, V_{PI} is the volume of the three I blocks in the miktoarm star block copolymer and f_{PI} is the volume fraction of the I phase at the particular hPS blend composition. For long hPS chains, we found that the value is approximately equal to 15.8 nm^2 for each molecule and is nearly constant at different hPS fractions, up until the complete unbinding transition of the lamellae (fit line in Figure 3b). Indeed, the long hPS molecules cannot penetrate into the S domains, yielding "dry" brush conditions. In comparison, the short hPS (20.8 kg/mol) chains penetrate into the "wet" S brushes near the S/I interface and thus the average area per chain expands considerably with increasing hPS fraction. This overabundance of area per copolymer is ultimately relieved at the OOT with a spontaneous change in interfacial curvature to produce discrete I and continuous S domains.

In summary, the unusual $S(IS')_3$ miktoarm star block architecture evidently stabilizes extremely asymmetric lamellar structures to high degrees of swelling in binary blends with hPS. The molecular weight of the hPS relative to the S and S′ blocks of the miktoarm is critical: long hPS chains produce macrophase separation, while short hPS chains facilitate order–order transitions. Intermediate length hPS renders asymmetric lamellae stable over a broad range of compositions, although the lamellae lose positional and orientational order through defect creation and unbinding when swollen to high extents. The domain features are tunable between 37 nm and several hundred nanometers, which affords a flexible and efficient platform for future applications of asymmetric lamellar structures. Notably, although this study was conducted with styrene/isoprene systems, the general principles deduced

DOI: 10.1021/jacs.5b02881
J. Am. Chem. Soc. 2015, 137, 6160−6163

provide a guiding protocol to other chemical constitutions with more versatile functionalities.

■ ASSOCIATED CONTENT

Supporting Information

Part A: Synthesis method and molecular characterization; Part B: Sample preparation and characterization methods; Part C: TEM images for blends with 20.8 kg/mol hPS; Part D: TEM images for blends with 136 kg/mol hPS; Part E: Small angle synchrotron X-ray scattering data; Part F: PS, PI layer thickness; Part G: Interfacial thickness; Part H: Brief introduction to SCFT method. The Supporting Information is available free of charge on the ACS Publications website at DOI: 10.1021/jacs.5b02881.

■ AUTHOR INFORMATION

Corresponding Authors

*ghf@mrl.ucsb.edu

*aavger@cc.uoi.gr

Notes

The authors declare no competing financial interest.

△Deceased, December 27, 2014.

■ ACKNOWLEDGMENTS

This research was supported by the Institute for Collaborative Biotechnologies through grant W911NF-09-0001 from the U.S. Army Research Office. The content of the information does not necessarily reflect the position or the policy of the Government, and no official endorsement should be inferred. Extensive use was made of the MRL Shared Experimental Facilities supported by the MRSEC Program of the NSF under award no. DMR 1121053; a member of the NSF-funded Materials Research Facilities Network (www.mrfn.org). We also acknowledge support from the Center for Scientific Computing at the CNSI and MRL: an NSF MRSEC (DMR-1121053) and NSF CNS-0960316.

■ REFERENCES

(1) Gozen, B. A.; Tabatabai, A.; Ozdoganlar, O. B.; Majidi, C. *Adv. Mater.* **2014**, *26*, 5211.

(2) Moonen, P. F.; Yakimets, I.; Huskens, J. *Adv. Mater.* **2012**, *24*, 5526.

(3) Lee, J.-H.; Koh, C. Y.; Singer, J. P.; Jeon, S.-J.; Maldovan, M.; Stein, O.; Thomas, E. L. *Adv. Mater.* **2014**, *26*, 532.

(4) Mitov, M. *Adv. Mater.* **2012**, *24*, 6260.

(5) Kang, C.; Kim, E.; Baek, H.; Hwang, K.; Kwak, D.; Kang, Y.; Thomas, E. L. *J. Am. Chem. Soc.* **2009**, *131*, 7538.

(6) Macfarlane, R. J.; Kim, B.; Lee, B.; Weitekamp, R. A.; Bates, C. M.; Lee, S. F.; Chang, A. B.; Delaney, K. T.; Fredrickson, G. H.; Atwater, H. A.; Grubbs, R. H. *J. Am. Chem. Soc.* **2014**, *136*, 17374.

(7) Carlson, A.; Bowen, A. M.; Huang, Y.; Nuzzo, R. G.; Rogers, J. A. *Adv. Mater.* **2012**, *24*, 5284.

(8) Bates, F. S.; Hillmyer, M. A.; Lodge, T. P.; Bates, C. M.; Delaney, K. T.; Fredrickson, G. H. *Science* **2012**, *336*, 434.

(9) Kim, J. K.; Han, C. D. *Adv. Polym. Sci.* **2010**, *231*, 77.

(10) (a) Matsen, M. W. *Macromolecules* **2012**, *45*, 2161. (b) Matsen, M. W. *J. Chem. Phys.* **2000**, *113*, 5539.

(11) Leibler, L. *Macromolecules* **1980**, *13*, 1602.

(12) Khandpur, A. K.; Förster, S.; Bates, F. S.; Hamley, I. W.; Ryan, A. J.; Bras, W.; Almdal, K.; Mortensen, K. *Macromolecules* **1995**, *28*, 8796.

(13) Winey, K. I.; Thomas, E. L.; Fetters, L. J. *Macromolecules* **1991**, *24*, 6182.

(14) Mayes, A. M.; Russell, T. P.; Satija, S. K.; Majkrzak, C. F. *Macromolecules* **1992**, *25*, 6523.

(15) (a) Koizumi, S.; Hasegawa, H.; Hashimoto, T. *Macromolecules* **1994**, *27*, 7893. (b) Kimishima, K.; Hashimoto, T.; Han, C. D. *Macromolecules* **1995**, *28*, 3842.

(16) Matsen, M. W. *Phys. Rev. Lett.* **1995**, *74*, 4225.

(17) Leibler, L. *Makromol. Chem., Macromol. Symp.* **1988**, *16*, l.

(18) (a) Han, S. H.; Pryamitsyn, V.; Bae, D.; Kwak, J.; Ganesan, V.; Kim, J. K. *ACS Nano* **2012**, *6*, 7966. (b) Valkama, S.; Kosonen, H.; Ruokolainen, J.; Haatainen, T.; Torkkeli, M.; Serimaa, R.; Brinke, G. ten; Ikkala, O. *Nat. Mater.* **2004**, *3*, 872.

(19) Walther, A.; André, X.; Drechsler, M.; Abetz, V.; Müller, A. H. E. *J. Am. Chem. Soc.* **2007**, *129*, 6187.

(20) Widin, J. M.; Schmitt, A. K.; Schmitt, A. L.; Im, K.; Mahanthappa, M. K. *J. Am. Chem. Soc.* **2012**, *134*, 3834.

(21) (a) Court, F.; Hashimoto, T. *Macromolecules* **2001**, *34*, 2536. (b) Court, F.; Yamaguchi, D.; Hashimoto, T. *Macromolecules* **2008**, *41*, 4828. (c) Chen, F.; Kondo, Y.; Hashimoto, T. *Macromolecules* **2007**, *40*, 3714.

(22) Milner, S. T. *Macromolecules* **1994**, *27*, 2333.

(23) Matsen, M. W.; Schick, M. *Macromolecules* **1994**, *27*, 6761.

(24) Dyer, C.; Driva, P.; Sides, S. W.; Sumpter, B. G.; Mays, J. W.; Chen, J.; Kumar, R.; Goswami, M.; Dadmun, M. D. *Macromolecules* **2013**, *46*, 2023.

(25) Beyer, F. L.; Gido, S. P.; Velis, G.; Hadjichristidis, N.; Tan, N. B. *Macromolecules* **1999**, *32*, 6604.

(26) (a) Avgeropoulos, A.; Dair, B. J.; Thomas, E. L.; Hadjichristidis, N. *Polymer* **2002**, *43*, 3257. (b) Avgeropoulos, A.; Hadjichristidis, N. *J. Polym. Sci., Part A: Polym. Chem.* **1997**, *35*, 813.

(27) Lynd, N. A.; Oyerokun, F. T.; O'Donoghue, D. L.; Handlin, D. L., Jr.; Fredrickson, G. H. *Macromolecules* **2010**, *43*, 3479.

(28) Shi, W.; Lynd, N. A.; Montarnal, D.; Luo, Y.; Fredrickson, G. H.; Kramer, E. J.; Ntaras, C.; Avgeropoulos, A.; Hexemer, A. *Macromolecules* **2014**, *47*, 2037.

(29) (a) Lipowsky, R.; Leibler, S. *Phys. Rev. Lett.* **1987**, *56*, 2541. (b) Netz, R.; Lipowsky, R. *Phys. Rev. Lett.* **1993**, *71*, 3596. (c) Milner, S. T.; Roux, D. *J. Phys. I (France)* **1992**, *2*, 1741.

(30) Delaney, K. T.; Fredrickson, G. H. *Comput. Phys. Commun.* **2013**, *184*, 2102.

(31) Fredrickson, G. H. *The Equilibrium Theory of Inhomogeneous Polymers*; Clarendon: Oxford, 2006.

(32) Nelson, D. R.; Toner, J. *Phys. Rev. B* **1981**, *24*, 363.

(33) Vogel, M.; Münster, C.; Fenzl, W.; Salditt, T. *Phys. Rev. Lett.* **2000**, *84*, 390.

(34) (a) Milner, S. T.; Witten, T. A.; Cates, M. E. *Macromolecules* **1988**, *21*, 2610. (b) Milner, S. T.; Witten, T. A.; Cates, M. E. *Macromolecules* **1989**, *22*, 853. (c) Hadjichristidis, N.; Iatrou, H.; Behal, S. K.; Chludzinski, J. J.; Disko, M. M.; Garner, R. T.; Liang, K. S.; Lohse, D. J.; Milner, S. T. *Macromolecules* **1993**, *26*, 5812. (d) Pochan, D. J.; Gido, S. P.; Pispas, S.; Mays, J. W.; Ryan, A. J.; Fairclough, J. P. A.; Hamley, I. W.; Terrill, N. J. *Macromolecules* **1996**, *29*, 5091.

DOI: 10.1021/jacs.5b02881
J. Am. Chem. Soc. 2015, 137, 6160−6163